Research Experience

Yijun Wang

Nanjing University, China

Homepage: https://yijunyuxuan.github.io/WangYijun.github.io/
Email: wangyijun@nju.edu.cn

Contents

1 Activities of radio AGNs: from accretion disc to large-scale environment (Postdoc in Nanjing University, 2021-)

1.1 Central engines of radio AGNs

The fundamental plane of black hole activity describes the correlation between radio luminosity ($L_{\rm R}$), X-ray luminosity ($L_{\rm X}$), and black hole mass ($M_{\rm BH}$). It reflects a connection between the accretion disc and the jet. However, this relationship shows a large scatter for active galactic nuclei (AGN). Based on a sample consisting of 208 low-luminosity AGN from COSMOS, GOODS-N, and GOODS-S fields, we confirm the conclusion found in previous works, which demonstrates that the scatter of fundamental plane is related to radio-loudness, and **we additionally found that the scatter of fundamental plane is also related to the Eddington ratio and the star formation properties of host galaxies. These results also provide an implication about the central engines of radio-quiet and radio-loud AGNs.**

ADS link: https://ui.adsabs.harvard.edu/abs/2024A%26A...689A.327W/abstract

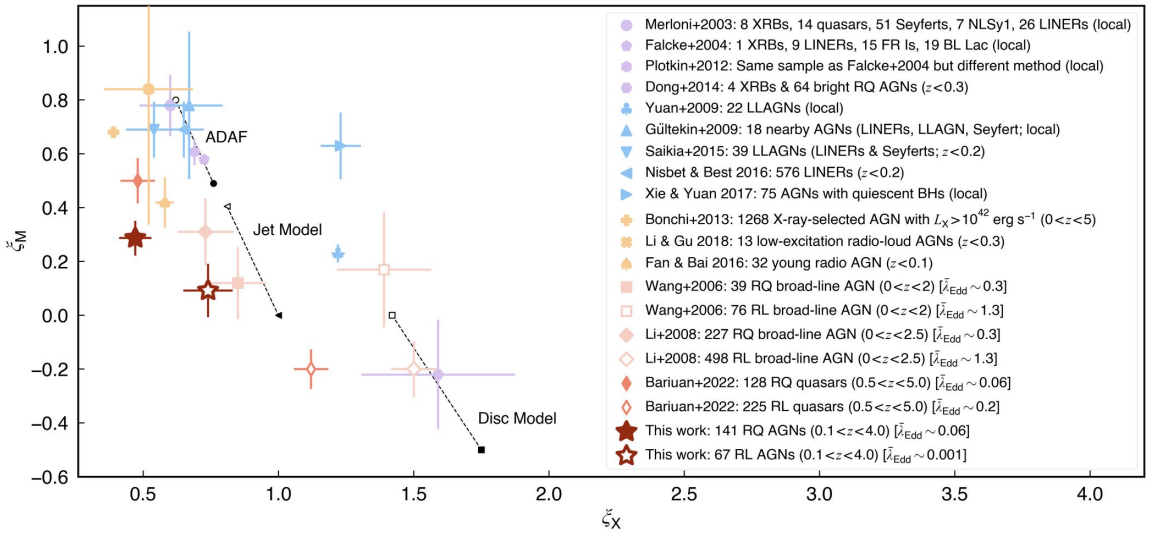

Figure 1: Comparison of the best-fit correlation coefficients, ξ_X and ξ_M, of the fundamental plane. The fundamental plane of black hole activity is defined as $\log L_{\rm R} = \xi_{\rm X} \log L_{\rm X} + \xi_{\rm M} M_{\rm BH} + b$ where $L_{\rm R}$ is the rest-frame 5 GHz radio luminosity, $L_{\rm X}$ is the rest-frame 2–10 keV X-ray luminosity, and $M_{\rm BH}$ is the black hole mass.

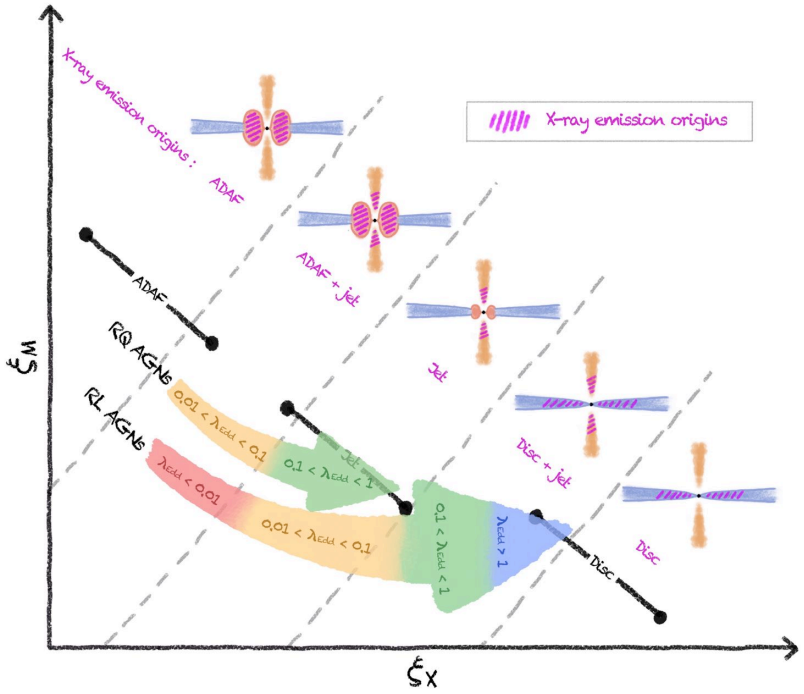

Figure 2: Cartoon illustrating the model for the central engine of radio-quiet (RQ) AGNs and radio-loud (RL) AGNs.

1.2 Host galaxies of radio AGNs

Radio-excess active galactic nuclei (radio-AGNs) are essential to our understanding of both the physics of black hole (BH) accretion and the interaction between BHs and host galaxies. Thanks to recent deep and wide radio continuum surveys, we make the studies about radio-AGNs down to lower luminosities and up to higher redshifts than previous studies based on 983 radio-AGNs at $0 < z < 4$ from COSMOS and GOODS-N fields. We derived the turnover luminosity ($L_{\rm D}$), above which the number density of radio-AGNs surpasses that of star forming galaxies (SFGs). **The evolution of $L_{\rm D}$ follows $L_{\rm D} = 10^{22.9} \times (1+z)^{0.06\times z+3.05}$, which increases from $10^{22.9}$ W Hz^{-1} at $z \sim 0$ to $10^{25.2}$ W Hz^{-1} at $z \sim 4$. This relation provides us with another way to select powerful radio-AGNs at different redshifts solely through radio survey. We further derive the probability ($p_{\rm radio}$) of SFGs and quiescent galaxies (QGs) hosting a radio-AGN, as a function of stellar mass ($M_\star$), radio luminosity ($L_{\rm R}$), and redshift (z), which yields $p_{\rm radio} \propto (1+z)^{3.08}\ M_\star^{1.06}\ L_{\rm R}^{-0.77}$ for SFGs, and $p_{\rm radio} \propto (1+z)^{2.47}\ M_\star^{1.41}\ L_{\rm R}^{-0.60}$ for QGs, respectively.**

ADS link: https://ui.adsabs.harvard.edu/abs/2024A%26A...685A..79W/abstract

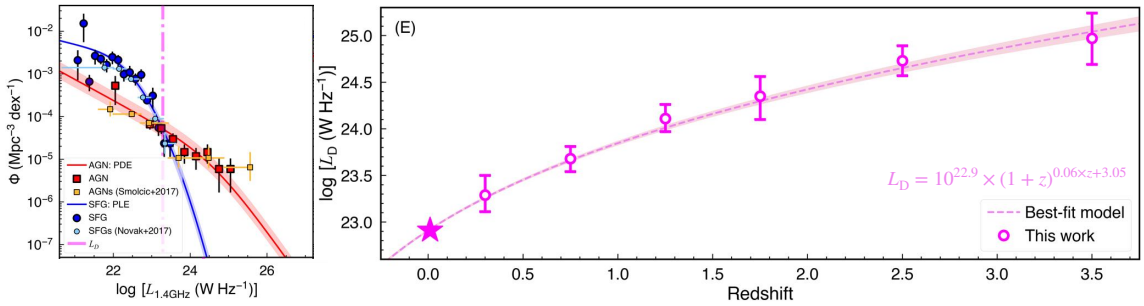

Figure 3: 1.4 GHz radio luminosity function of SFGs (blue circles) and radio-excess AGNs (red squares) (left panel) and evolution of turnover luminosity ($L_{\rm D}$) above which the number density of radio-AGNs surpasses that of SFGs ($L_{\rm D}$) (right panel).

1.3 Effects of radio AGNs on satellites in galaxy groups (to be submitted)

Radio AGNs are usually thought to perform the most efficient feedback on their host galaxies and surrounding environments. However, it is still unclear how do radio AGNs affect the star formation properties of their satellites. Based on a large galaxy group sample from X. Yang et al. (2007), we found that central galaxies hosting a radio AGN have higher quenched satellite fraction than central galaxies being a normal galaxy with redshift, halo mass, stellar mass of central galaxies, star formation rate of central galaxies, and black hole mass of central galaxies being controlled. Central galaxies hosting an Fanaroff-Riley Class II source have even higher quenched satellite fraction. **These results indicate that radio AGNs and large-scale radio lobes significantly quenched the star formation in satellites, which might be one origin of the galactic conformity.**

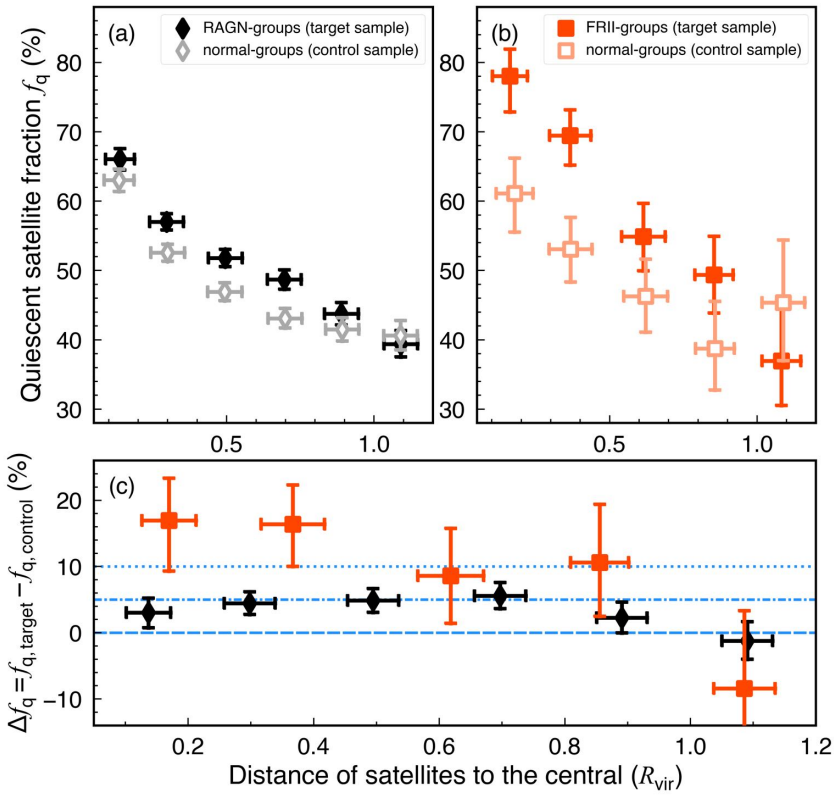

Figure 4: Quenched satellite fraction plotted against distance to the central galaxies (in the unit of virial radius). Target sample is composed of galaxy groups whose central galaxies are radio AGNs (RAGN-groups; black diamonds) or FRII sources (FRII-groups; red circles). Control sample consists of galaxy groups whose central galaxies are normal galaxies (normal-groups). The halo mass of galaxy groups, redshift of central galaxies, stellar mass of central galaxies, star formation rate of central galaxies, and black hole mass of central galaxies between target and control samples are matched.

2 Relationship between jets and outflows in AGN (Postdoc in Nanjing University, 2021-)

2.1 Host galaxy of radio-loud AGN 3C 59

We report a rare case where an elliptical radio-loud quasar host, 3C 59, rejuvenates star formation activity through minor mergers with its nearby satellite galaxies. The inferred star formation history of 3C 59 shows significant star formation rejuvenation within the past 500 Myr, before which remains rather quiescent for most of the cosmic time. In addition, through the image decomposition for DESI images, we obtained the AGN fluxes at g, r, and z bands, which are utilized in the following analysis for warm absorbers outflows.

ADS link: https://ui.adsabs.harvard.edu/abs/2025ApJ...980..107W/abstract

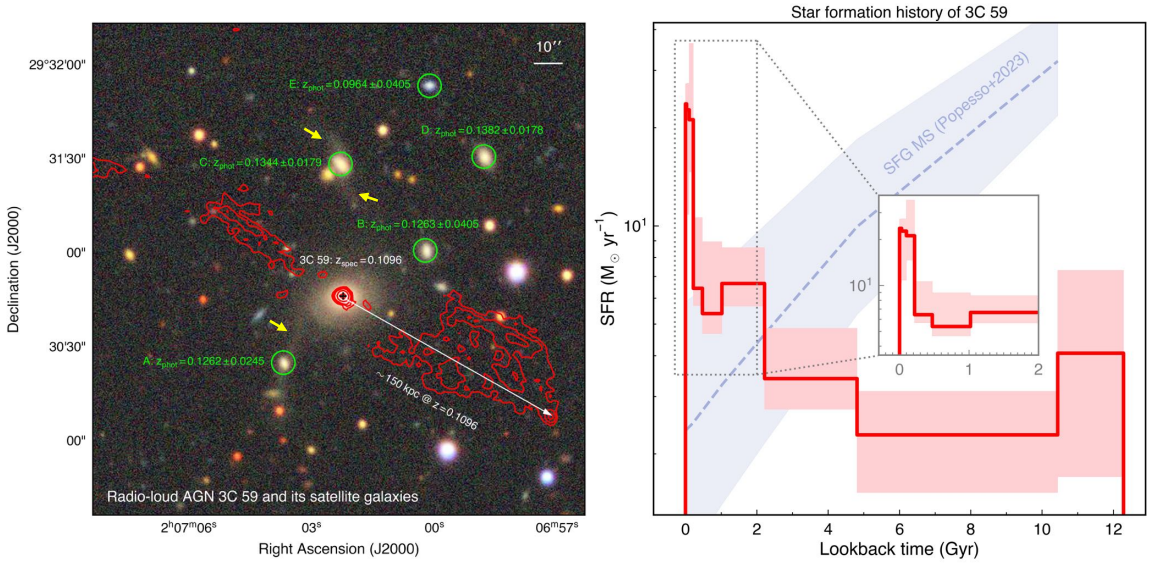

Figure 5: Images for 3C 59 (the black cross) and its five satellite galaxies (A, B, C, D, and E; the green circles) (left panel), and the star formation history of 3C 59 (right panel).

2.2 Warm absorber outflows in 3C 59 (in press)

Both jets and ionized outflows in active galactic nuclei (AGNs) are thought to play important roles in affecting the star formation and evolution of host galaxies, but their relationship is still unclear. As a pilot study, we performed a detailed spectral analysis for a radio-loud (RL) AGN 3C 59 ($z = 0.1096$). 3C 59 is one rare target for simultaneously studying jets and warm absorbers that is one type of ionized outflows. We found two warm absorbers with ionization parameter of $\log[\xi/(\mathrm{erg\ cm\ s^{-1}})] = 2.65^{+0.10}_{-0.09}$ and 1.65 ± 0.11, respectively, and their outflowing velocities are $v_{\rm out} = -528^{+163}_{-222}$ km s^{-1} and -228^{+121}_{-122} km s^{-1}, respectively. Their positive $v_{\rm out}$-ξ relation can be explained by the radiation-pressure-driven mechanism. **We present a comparative study of outflow driven mechanism between a RL AGN (3C 59) and a radio-quiet AGN (NGC 3227), which suggests a similar driven mechanism of their warm absorber outflows and a negligible role of jets in this process.**

ADS link: https://ui.adsabs.harvard.edu/abs/2025arXiv251006752W/abstract

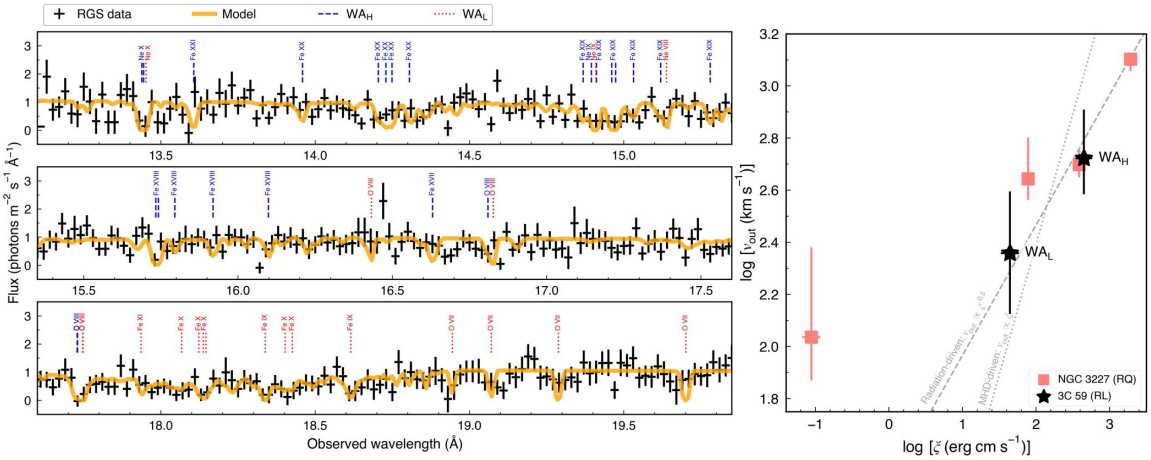

Figure 6: The 13–20 Å RGS spectrum with main absorption features produced by the warm absorbers ($\mathrm{WA_H}$ and $\mathrm{WA_L}$) of 3C 59 (left panels) and outflowing velocity ($v_{\rm out}$) plotted against ionization parameter (ξ) (right panels).

3 Density profile of ambient circumnuclear medium in Seyfert galaxies (Postdoc in Nanjing University, 2021-)

The shape of the ambient circumnuclear medium (ACM) density profile can probe the history of accretion onto the central supermassive black holes in galaxies and the circumnuclear environment. However, due to the limitations of instrument resolution, the density profiles of the ACM for most galaxies remain largely unknown. **We propose a novel method to measure the ACM density profile of active galactic nuclei (AGNs) by the equilibrium between the radiation pressure on the warm absorbers (WAs, a type of AGN outflow) and the drag pressure from the ACM.** We study the correlation between the outflow velocity and ionization parameter of WAs in each of the five Seyfert 1 galaxies (NGC 3227, NGC 3783, NGC 4051, NGC 4593, and NGC 5548), inferring that the density profile of the ACM is between $n \propto r^{-1.7}$ and $n \propto r^{-2.15}$ (n is number density and r is distance) from 0.01 pc to parsec scales in these five AGNs. Our results indicate that the ACM density profile in Seyfert 1 galaxies is steeper than the prediction by the spherically symmetric Bondi accretion model and the simulated results of the hot accretion flow, but more in line with the prediction by the standard thin-disk model.

ADS link: https://ui.adsabs.harvard.edu/abs/2022ApJ...928....7W/abstract

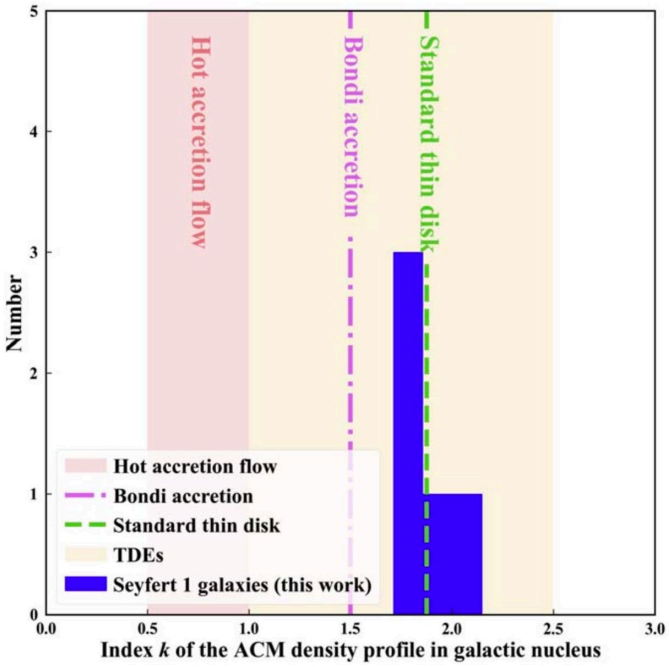

Figure 7: The distribution of the ACM density profile index k for the five Seyfert 1 galaxies (NGC 3227, NGC 4051, NGC 4593, NGC 5548, and NGC 3783; blue histogram). The ACM density profile is defined as $n \propto r^{-k}$ where r is the radial distance of the absorbing gas to the central engine.

4 Transient obscuration event captured in NGC 3227 (Joint-supervision PhD students in Leiden University, 2019-2020)

4.1 Continuum model for the broadband spectral energy distribution (as a collaborator)

From Swift monitoring of a sample of active galactic nuclei (AGN) we found a transient X-ray obscuration event in Seyfert-1 galaxy NGC 3227, and thus triggered our joint XMM-Newton, NuSTAR, and Hubble Space Telescope (HST) observations to study this event. **Here in the first paper of our series we present the broadband continuum modelling of the spectral energy distribution for NGC 3227, extending from near infrared (NIR) to hard X-rays.** We use our new spectra taken with XMM-Newton, NuSTAR, and the HST Cosmic Origins Spectrograph in 2019, together with archival unobscured XMM-Newton, NuSTAR, and HST Space Telescope Imaging Spectrograph data, in order to disentangle various spectral components of NGC 3227 and recover the underlying continuum.

ADS link: https://ui.adsabs.harvard.edu/abs/2021A%26A...652A.150M/abstract

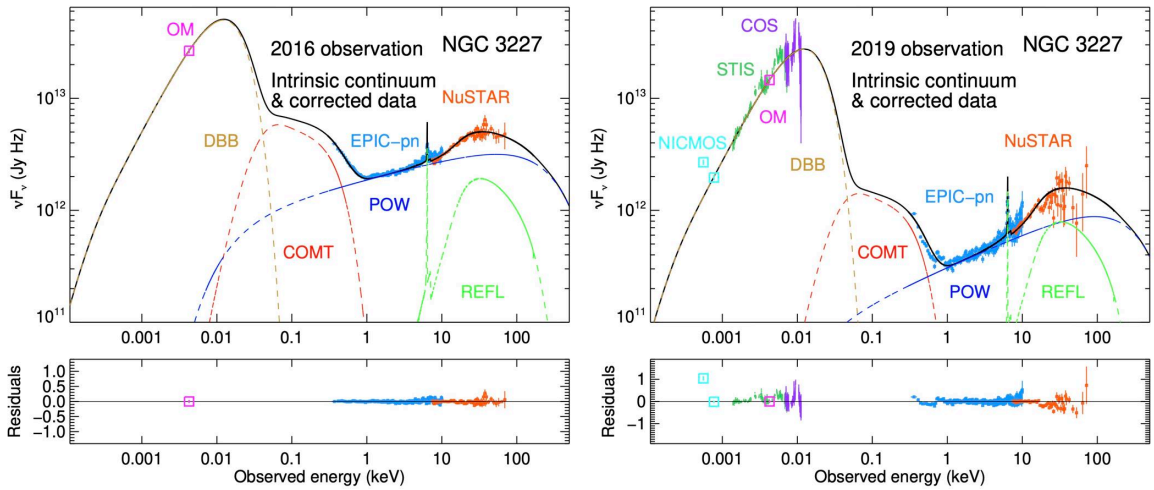

Figure 8: SED continuum model of NGC 3227 from NIR to hard X-rays.

4.2 Warm absorbers and obscuration events in 2006 and 2016

The relationship between warm absorber (WA) outflows of active galactic nuclei and nuclear obscuration activities caused by optically thick clouds (obscurers) crossing the line of sight is still unclear. NGC 3227 is a suitable target for studying the properties of both warm absorber (WA) and obscurers. In the aim of investigating WAs and obscurers of NGC 3227 in detail, we used a broadband spectral-energy-distribution model that is built in findings of the first paper in our series together with the photoionization code of SPEX software to fit the archival observational data taken by XMM-Newton and NuSTAR in 2006 and 2016. It is worth noting that we find an X-ray obscuration event in the beginning of the 2006 observation, which was missed by previous studies. **The obscurers of NGC 3227 are closer to the center and have larger number densities than the WAs, which indicates that the WAs and obscurers might have different origins.**

ADS link: https://ui.adsabs.harvard.edu/abs/2022A%26A...657A..77W/abstract

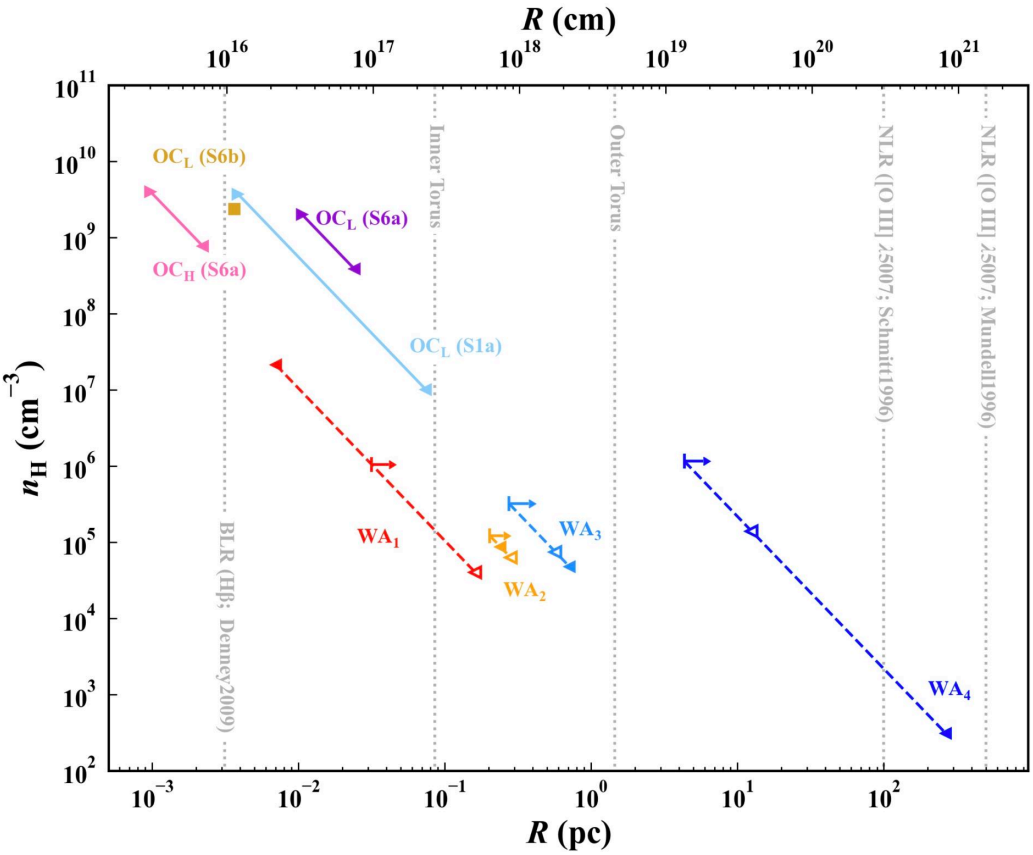

Figure 9: Distances of the four WAs (WA_1, WA_2, WA_3, WA_4) and four obscurer components (OC) from the center of NGC 3227.

4.3 Photoionization modeling of the X-ray obscuration event in 2019 (as a collaborator)

Multiple X-ray obscuration events were reported in the nearby Seyfert 1.5 galaxy NGC 3227 from 2000 to 2016. In late 2019, another X-ray obscuration event was identified with Swift. We aim to constrain the physical properties of the absorbing material (i.e., the obscurer) that caused the X-ray obscuration event in late 2019. We also aim to compare the handful of obscuration events in NGC 3227 and other Seyfert galaxies. We performed photoionization modeling with the SPEX code, which allows us to constrain the intrinsic continuum simultaneously with various photoionized absorption and emission components. Similar to previous transient X-ray obscuration events in NGC 3227, the one caught in late 2019 is short-lived (less than five months). **Unlike some other X-ray obscuration events in Seyfert galaxies, such as NGC 5548 and NGC 3783, no prominent blueshifted, broad absorption troughs were found in the 2019 HST/COS spectra of NGC 3227 when compared with archival UV spectra. This might be explained if the X-ray obscurer does not intercept our line of sight to (a significant portion of) the UV-emitting region.**

ADS link: https://ui.adsabs.harvard.edu/abs/2022A%26A...665A..72M/abstract

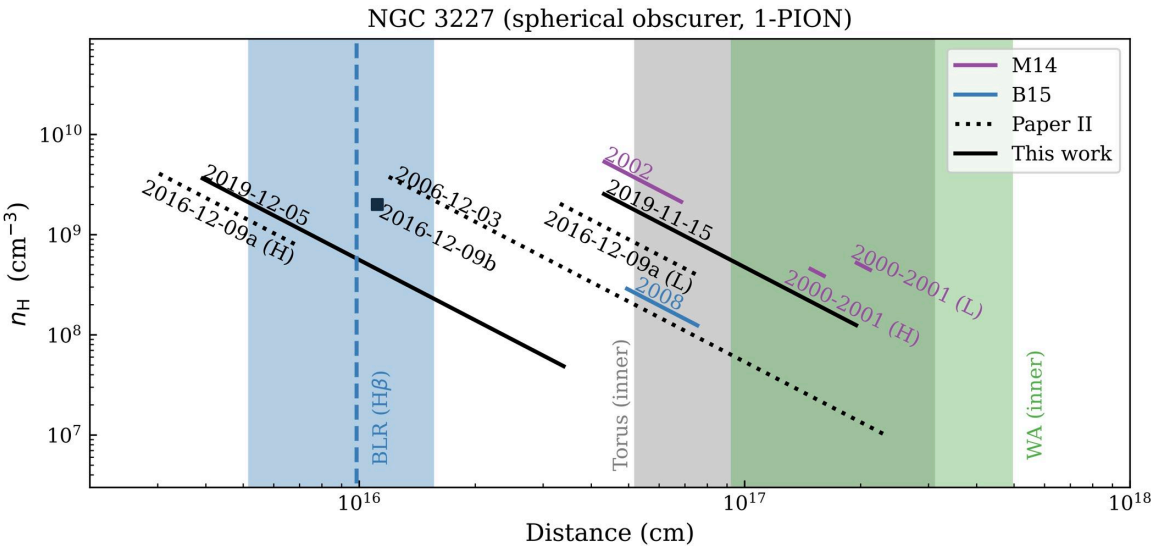

Figure 10: Distance and number density (n_H) of obscurers in NGC 3227.

4.4 Origin of the obscuring cloud variability (as a collaborator)

We aim to determine the nature and origin of the observed spectral variability in the 2019 obscuration event. We study the evolution of the obscurer by splitting the two XMM-Newton observations from 2019 into timing bins of length ∼10 ks. We used the SPEX code to analyze the 0.35–10 keV EPIC-PN spectra of each timing bin. In the first observation (Obs 1), there is a strong anti-correlation between the column density ($N_{\rm H}$) of the obscurer and the continuum normalizations of the X-ray power law and soft Comptonization components ($N_{\rm pow}$ and $N_{\rm comt}$, respectively). The second observation (Obs 2) displays a significantly lower count rate due to the combination of a high NH and covering fraction of the obscurer, and a lower continuum flux. **The observed variability seen during the obscuration event of NGC 3227 in 2019 is likely driven by the continuum, but the obscurer varies at the same time, making it difficult to distinguish between the two possibilities with full certainty.**

ADS link: https://ui.adsabs.harvard.edu/abs/2023A%26A...673A..26G/abstract

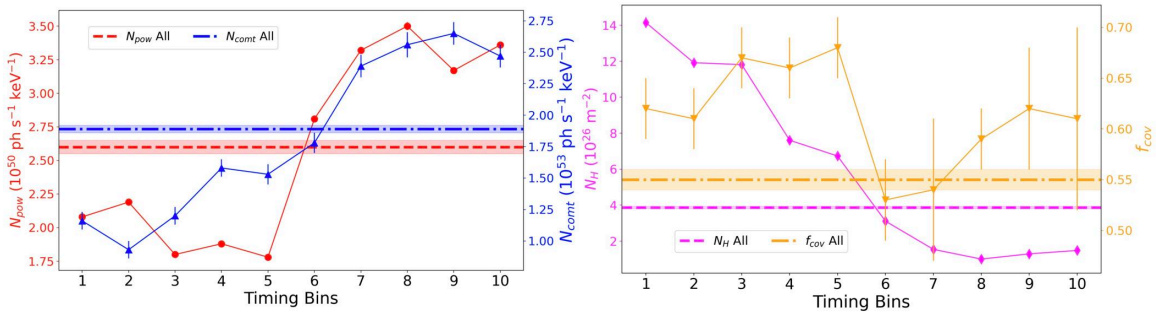

Figure 11: Further tests to determine the cause of the observed variability.

5 X-ray variabilities in blazars (PhD students in University of Science and Technology of China, 2014-2019)

5.1 Systematic Investigation of X-Ray Spectral Variability of TeV Blazars during Flares in the RXTE Era

Utilizing all the 16 yr RXTE observations, we analyze the X-ray spectra of 32 TeV blazars and perform a systematic investigation of X-ray spectral variability for the five brightest sources during their major flares that lasted several days. We obtain photon spectral index (α), flux and synchrotron radiation peak energy ($E_{\rm p}$) from empirical spectral fitting, and electron spectral index (p) from theoretical synchrotron radiation modeling. We find that both α and p generally display a harder-when-brighter trend, confirming the results of many previous works. Furthermore, **we confirm and strengthen the result that p must vary in order to explain the observed X-ray spectral variability during flares, which would have useful implications for interpreting the associated higher-energy spectral variability. When considering TeV blazars as a whole, α and X-ray luminosity are positively correlated, $E_{\rm p}$ is negatively correlated with p and α, and $E_{\rm p}$ is positively correlated with HR; all these correlations are in line with the blazar sequence. However, after correcting for the Doppler boosting effect, α and intrinsic X-ray luminosity follow an anti-correlation.**

ADS link: https://ui.adsabs.harvard.edu/abs/2018ApJ...867...68W/abstract

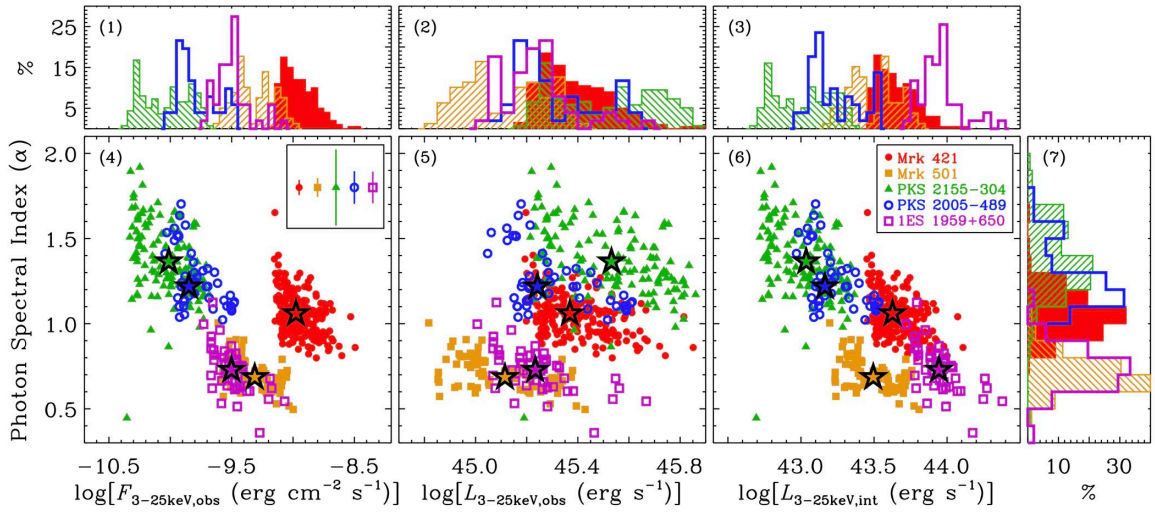

Figure 12: Relations between photon spectral index (α) and brightness parameters: observed 3–25 keV X-ray flux ($F_{\rm 3–25keV,obs}$; panel (4)), observed luminosity ($L_{\rm 3–25keV,obs}$; panel (5)), and intrinsic luminosity ($L_{\rm 3–25keV,int}$, which has been corrected for the Doppler boosting effect; panel (6)) for the five sources, respectively.

5.2 X-Ray Spectral Variations of Synchrotron Peak in BL Lacs

The spectral energy distribution of blazars around the synchrotron peak can be well described by the log-parabolic model that has three parameters: peak energy ($E_{\rm p}$), peak luminosity ($L_{\rm p}$), and the curvature parameter (b). It has been suggested that $E_{\rm p}$ shows relations with $L_{\rm p}$ and b in several sources, which can be used to constrain the physical properties of the emitting region and/or acceleration processes of the emitting particles. We systematically study the $E_{\rm p}$–$L_{\rm p}$ and $E_{\rm p}$–$(1/b)$ relations for 14 BL Lac objects using the 3–25 keV RXTE/PCA and 0.3–10 keV Swift/XRT data. Most objects (9/14) exhibit positive $E_{\rm p}$–$L_{\rm p}$ correlations, three sources show no correlation, and two sources display negative correlations. In addition, most targets (7/14) present no correlation between $E_{\rm p}$ and $1/b$, five sources pose negative correlations, and two sources demonstrate positive correlations. 1ES 1959+650 displays two different $E_{\rm p} - L_{\rm p}$ relations in 2002 and 2016. We also analyze $E_{\rm p}$–$L_{\rm p}$ and $E_{\rm p}$–$(1/b)$ relations during flares lasting for several days. The $E_{\rm p}$–$L_{\rm p}$ relation does not exhibit significant differences between flares, while the $E_{\rm p}$–$(1/b)$ relation varies from flare to flare. **For the total sample, when $L_{\rm p} < 10^{45}$ erg s^{-1}, there seems to be a positive $E_{\rm p}$–$L_{\rm p}$ correlation. $L_{\rm p}$ and the slope of $E_{\rm p}$–$L_{\rm p}$ relation present an anti-correlation, which indicates that the causes of spectral variations might be different between luminous and faint sources.**

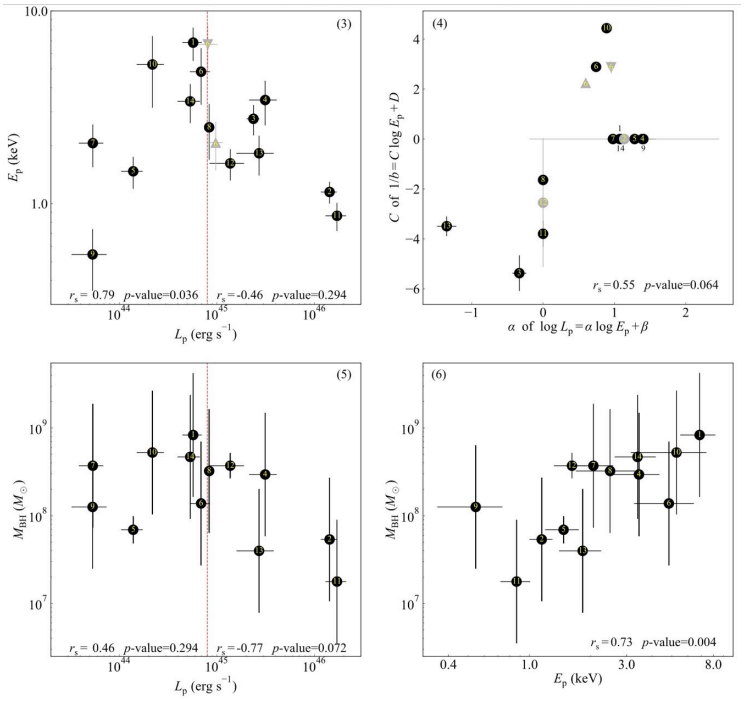

Figure 13: Correlations between $E_{\rm p}$ and $L_{\rm p}$ (panel 3), between C and α (panel 4), between $M_{\rm BH}$ and $L_{\rm p}$ (panel 5), and between $M_{\rm BH}$ and $E_{\rm p}$ (panel 6) for the 14 sources in the total sample.

6 Publication list

1 **Yijun Wang**, Tao Wang, Junjie Mao, Yerong Xu, Zhicheng He, Zheng Zhou, Chen Li, Yongquan Xue, Jiayi Chen, Fangzheng Shi, Missagh Mehdipour, 2025, A&A (in press), "Warm absorber outflows in radio-loud active galactic nucleus 3C 59"

2 **Yijun Wang**, Tao Wang, Ke Xu, Junjie Mao, Yerong Xu, Zheng Zhou, 2025, ApJ, "Minor-merger-induced star formation rejuvenation in an elliptical radio-loud quasar host, 3C 59"

3 **Yijun Wang**, Tao Wang, Luis C. Ho, Yuxing Zhong, Bin Luo, 2024, A&A, "The fundamental plane of black hole activity for low-luminosity radio active galactic nuclei across $0 < z < 4$"

4 **Yijun Wang**, Tao Wang, Daizhong Liu, Mark T. Sargent, Fangyou Gao, David M. Alexander, Wiphu Rujopakarn, Luwenjia Zhou, Emanuele Daddi, Ke Xu, Kotaro Kohno, Shuowen Jin, 2024, A&A, "Cosmic evolution of radio-excess active galactic nuclei in quiescent and star-forming galaxies across $0 < z < 4$"

5 **Yijun Wang**, Zhicheng He, Junjie Mao, Jelle Kaastra, Yongquan Xue, and Mehdipour Missagh, 2022, ApJ, "Density profile of the ambient circumnuclear medium in Seyfert 1 galaxies"

6 **Yijun Wang**, Jelle Kaastra, Mehdipour Missagh, Junjie Mao, Elisa Costantini, Gerard A. Kriss, Ciro Pinto, Gabriele Ponti, Ehud Behar, Stefano Bianchi, Graziella Branduardi-Raymont, Barbara De Marco, Sam Grafton-Waters, Pierre Olivier Petrucci, Jacobo Ebrero, Dominic James Walton, Shai Kaspi, Yongquan Xue, Stáphane Paltani, Laura di Gesu, Zhicheng He, 2022, A&A, "Transient obscuration event captured in NGC 3227 II. Warm absorbers and obscuration events in archival XMM-Newton and NuSTAR observations"

7 **Yijun Wang**, Shifu Zhu, Yongquan Xue, Minfeng Gu, Shanshan Weng, and Huynh Anh N. Le, 2019, ApJ, "X-ray spectral variations of synchrotron peak in BL Lacs"

8 **Yijun Wang**, Yongquan Xue, Shifu Zhu, and Junhui Fan, 2018, ApJ, "Systematic investigation of X-ray spectral variability of TeV blazars during flares in the RXTE era"

9 **Yijun Wang**, Jelle de Plaa, 2023, Springer, Chapter "High-Resolution Spectral Analysis" in Book "High-Resolution X-ray Spectroscopy: Instrumentation, Data Analysis, and Science"

10 Fangyou Gao, Tao Wang, **Yijun Wang**, 2025, A&A, "An empirical model of the extragalactic radio background"

11 Zheng Zhou, Junjie Mao, Taotao Fang, **Yijun Wang**, Fabrizio Nicastro, Jiayi Chen, 2024, ApJ, "On the connection between the repeated X-ray quasiperiodic oscillation and warm absorber in the active galaxy RE J1034+396

12 Missagh Mehdipour, G. A. Kriss, Jelle Kaastra, **Yijun Wang**, Junjie Mao, Elisa Costantini, N. Arav, Ehud Behar, Stefano Bianchi, Graziella Branduardi-Raymont, M. Brotherton, M. Cappi, Barbara De Marco, Laura di Gesu, Jacobo Ebrero, Sam Grafton-Waters, Shai Kaspi, G. Matt, Stáphane Paltani, Pierre Olivier Petrucci, Ciro Pinto, Gabriele Ponti, F. Ursini, Dominic James Walton, 2021, A&A, "Transient obscuration event captured in NGC 3227. I. Continuum model for the broadband spectral energy distribution"

13 Other collaborative works: ADS link